Applied Geochemistry xxx (xxxx) xxx

Contents lists available at ScienceDirect

Applied Geochemistry

journal homepage: http://www.elsevier.com/locate/apgeochem

Extremely enrichment of ^{7}Li in highly weathered saprolites developed on granite from Huizhou, southern China

Jun-Wen Zhang [a], Zhi-Qi Zhao [b,*], Xiao-Dong Li [a], Ya-Ni Yan [b], Yun-Chao Lang [a], Hu Ding [a], Li-Feng Cui [a], Jun-Lun Meng [c], Cong-Qiang Liu [a,**]

[a] Institute of Surface-Earth System Science, School of Earth System Science, Tianjin University, Tianjin, 300072, China
[b] School of Earth Science and Resources, Chang'an University, Xi'an, 710054, China
[c] State Key Laboratory of Environmental Geochemistry, Institute of Geochemistry, Chinese Academy of Sciences, Guiyang, 550081, China

ARTICLE INFO

Editorial handling by Dr. Z Zimeng Wang

Keywords:
Lithium isotopes
Quartz
Granite
Chemical weathering

ABSTRACT

Lithium isotope is potentially useful tracer of continental weathering. However, the factors affecting Li isotope composition in highly weathered saprolites are still largely unclear. In the present study, Li and Nd isotope compositions in saprolites developed on granite from Huizhou, southern China, were analyzed and Li isotope composition in quartz samples separated from the saprolites was determined. The Nd isotope composition of saprolites ($\varepsilon_{Nd} = -6.1 \pm 0.4$, 1σ) was almost identical to that of parent granite ($\varepsilon_{Nd} = -5.7$), suggesting the eolian deposition in this profile is negligible. The $\delta^{7}Li$ value in saprolites varied greatly from −7.7‰ to +14.0‰. Below a depth of 3 m, almost all saprolites were isotopically lighter than the parent granite (+1.0‰). However, above 3 m, $\delta^{7}Li$ values were higher in saprolites (+2.2‰ to +14.0‰, average + 7.6‰) than in the parent granite and showed a significant increasing trend toward the surface. Moreover, the $\delta^{7}Li$ value showed a negative correlation with the CIA value below 3 m, but a positive correlation above 3 m. Compared with the parent granite, quartz separates had a higher Li concentration (1.1–28.9 mg/kg, average 9.5 mg/kg) and $\delta^{7}Li$ value (+12.1‰ to +13.9‰). As weathering progressed, the formation of secondary minerals (such as kaolinite) led to the incorporation of lighter ^{6}Li, which may have contributed significantly to the low $\delta^{7}Li$ value in saprolites below 3 m. However, this mechanism could not explain the relative enrichment of heavy ^{7}Li in the upper layer saprolites. The relative enrichment of quartz may contribute significantly to the increase of $\delta^{7}Li$ in saprolites. The direct evidence was that Li was abundant and distinctly isotopically heavier in quartz separates. Moreover, quartz content correlated positively with Li concentration ($R^2 = 0.90$, $p < 0.01$) and $\delta^{7}Li$ value ($R^2 = 0.90$, $p < 0.01$) in the upper layer saprolites. The results showed that a 10% increase in Li due to quartz enrichment ($\delta^{7}Li = \sim+13$‰) resulted in a +1.3‰ increase in $\delta^{7}Li$ in the saprolites. Our results highlight that relative enrichment of quartz may result in isotopically heavier Li in highly weathered saprolites developed on granite, which may help to explain the higher $\delta^{7}Li$ values detected near the surface layer of weathering profiles.

1. Introduction

Lithium and its isotopes are potentially useful tracers of continental weathering (Huh et al., 1998, 2001). Lithium is a fluid-mobile, moderately incompatible trace element in geochemical processes. It has two stable isotopes (7.5% ^{6}Li and 92.5% ^{7}Li) that have great mass-dependent fractionation potential in the terrestrial environment due to the large relative mass difference (~16%) existing between them. Similarly to other alkali metals, Li has only one redox state (+1 charge), so it is generally believed that its isotopic composition is not influenced by redox reactions. Moreover, compared with other non-traditional stable isotopes (such as B, Mg and Si), Li is not a nutrient, so its isotopic composition is not directly influenced by biological processes (e.g., Rudnick et al., 2004).

Lithium isotope composition ($\delta^{7}Li$) in terrestrial reservoirs varies greatly from −20‰ to +50‰ (Tomascak et al., 2016). Generally, Li in solids (silicate rocks, soils, river bedloads and suspended loads, etc.) is isotopically lighter than that in fluids (river water, groundwater,

* Corresponding author.
** Corresponding author.
E-mail addresses: zhaozhiqi@chd.edu.cn (Z.-Q. Zhao), liucongqiang@tju.edu.cn (C.-Q. Liu).

https://doi.org/10.1016/j.apgeochem.2020.104825
Received 25 September 2020; Received in revised form 6 November 2020; Accepted 10 November 2020
Available online 17 November 2020

seawater, etc.). This is mainly due to the tendency of heavy Li (^{7}Li) to enter fluids (high δ^7Li values) while ^{6}Li tends to be retained in solids during water-rock interactions (e.g., Kısakürek et al., 2005; Pogge von Strandmann et al., 2006). For the weathering process, the main mechanism of Li isotope fractionation involves ^{6}Li being preferentially incorporated into octahedral structures of newly formed secondary minerals (such as clays and hydroxides) (Pistiner and Henderson, 2003; Williams and Hervig, 2005; Vigier et al., 2008; Wimpenny et al., 2015; Hindshaw et al., 2019). As a result, the extent of Li isotope fractionation in saprolites depends on the type and amount of secondary minerals formed during silicate weathering (Liu et al., 2013; Pogge von Strandmann and Henderson, 2015). Based on this knowledge, it can be logically speculated that, as weathering progresses, Li in weathered products will gradually become isotopically lighter (lower δ^7Li values) than that in parent rock, due to the increased abundance of secondary minerals relative to primary minerals. This speculation is consistent with the decrease in the δ^7Li value in weathered products as the weathering intensity increases in weathering profiles (e.g., Rudnick et al., 2004). However, it is anomalous that the δ^7Li value shows an increasing trend (or shows no significant differences relative to the parent rock) in the top layer of most weathering profiles which have relatively high weathering intensities (Kısakürek et al., 2004; Huh et al., 2004; Lemarchand et al., 2010; Ryu et al., 2014; Li et al., 2020). This counterintuitive phenomenon has been explained in two ways. First, the input of externally-derived Li (such as eolian dust and marine aerosol) has relatively high δ^7Li values in the surface layer of the profile (e.g., Pistiner and Henderson, 2003; Kısakürek et al., 2004; Huh et al., 2004; Li et al., 2020). Second, Li isotope composition varies with the mineralogical and crystallographical evolution of the weathering profile, as well as with the kinetic isotope fractionation produced by Li diffusion in saprolites (Teng et al., 2010; Ryu et al., 2014). It must be noted that the factors affecting Li isotope compositions in highly weathered saprolites are still largely unclear and that this hinders our ability to understand the link between the Li isotope behavior and continental weathering.

In most crustal rocks, Li is mainly found in silicate minerals such as mica, feldspar, amphibole and pyroxene, as well as secondary clay minerals (e.g., chlorite). As a major rock-forming silicate mineral, quartz tends to have low concentrations of minor and trace elements compared with other rock-forming silicates. However, Li seems to be "enriched" and isotopically heavy in quartz. Studies have shown that, except for Al, Li is the most abundant metal element present in quartz (1–100 mg/kg) (Larsen et al., 2004; Lehmann et al., 2011). Moreover, relatively high Li content and high δ^7Li values have been observed in quartz from pegmatites (30–140 mg/kg and +14.7 to +21.3‰, respectively) (Teng et al., 2006a). These values are consistent with the results from other research that Li is abundant and isotopically heavy in quartz from granites (Li et al., 2018; Zhang et al., 2021a). Lithium is abundant in quartz because it can be incorporated into the quartz structure through a coupled substitution of Si^{4+} with $Li^{+}+Al^{3+}$ (Larsen et al., 2004). Therefore, in quartz, Li concentration is positively correlated with Al concentration (Lehmann et al., 2011). During the equilibrium isotope fractionation process, the heavier isotope is preferentially partitioned into sites that have the highest bond energy (e.g., Schauble, 2004). Thus, the heavy ^{7}Li prefers high-energy bonds, which are associated with low coordination number sites (two- or fourfold site) in quartz (Teng et al., 2006a, 2006b). Similarly, the relatively high δ^7Li value often found in fluids is partly related to Li^{+} forms tetrahedral coordination with four water molecules (Yamaji et al., 2001). In contrast, the lighter ^{6}Li is preferentially incorporated into minerals' octahedral structure (e.g., clays), which has a higher coordination number (Williams and Hervig, 2005; Wimpenny et al., 2015).

Quartz is relatively abundant and accounts for a high proportion (20%–45%) of rock-forming minerals in granite (e.g., Myers, 1997). Since quartz is a relatively inactive mineral during chemical weathering processes, compared with amphibole, mica, feldspar, etc., it is gradually enriched with granite weathering products as weathering progresses, except in case of extreme weathering intensity conditions (dissolution of quartz) (e.g., Liu et al., 2016). Previous studies on granitic weathering products showed that formation of secondary minerals and non-congruent dissolution of the parent rock could be the major causes of Li isotope fractionation during granite weathering (Rudnick et al., 2004; Lemarchand et al., 2010; Négrel and Millot, 2019).

Considering that Li is abundant and isotopically heavier in quartz, the variation of quartz content may also significantly affect Li composition in bulk saprolite samples. However, so far, previous studies of saprolites have not separately analyzed quartz, leaving of its influence on bulk samples data an open question. In the present study, highly weathered saprolites developed on granite were collected to evaluate the effect of formation of secondary minerals and changes in quartz content on Li isotope composition during granite weathering. In addition, the saprolite Nd isotope and rainwater Li isotope compositions were also analyzed to determine the effect of input of externally-derived (e.g., precipitation and eolian deposition) on Li isotope composition in upper layer saprolites.

2. Materials and methods

2.1. Sampling

Highly weathered saprolites developed on granite were collected from Huizhou, southern China (Fig. 1), where the mean annual temperature and mean annual precipitation are ~22 °C and ~1900 mm, respectively. The sampling site was located near the ridge of a mountain about 39 m above sea level and in close to proximity to the sea (about 57 km away). This granitic pluton was formed in the early Yanshanian and reports a zircon U–Pb age of about 140 Ma (Kuang et al., 2019).

Saprolites were obtained from a 6 m deep profile and did not reach the fresh granite. A total of fifteen saprolite samples were collected in April 2013 and veins were avoided during sampling. Before sampling, about 40 cm of saprolites on the vertical surface were peeled and

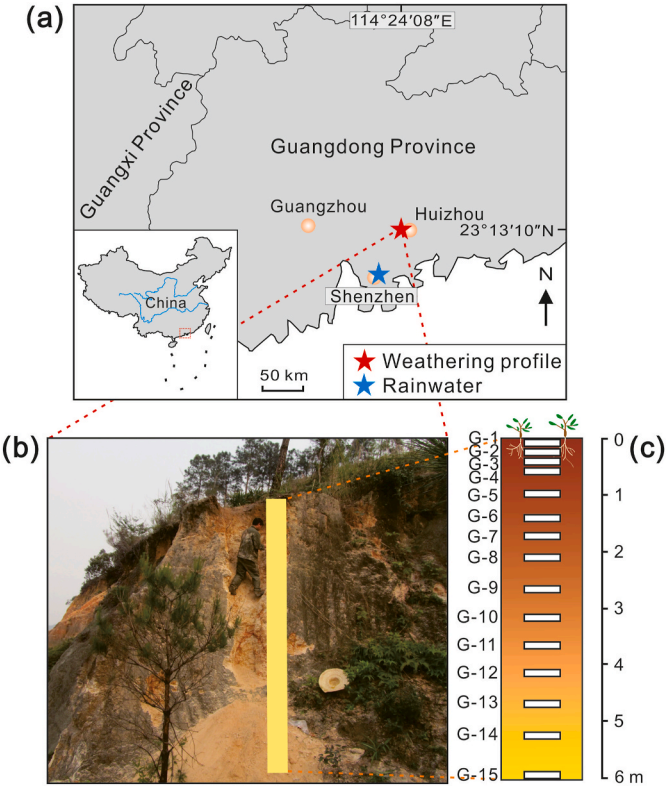

Fig. 1. Map of the sampling site: (a) the location of the sampling site; (b) the picture of the weathering profile; (c) the schematic diagram of sampling points.

discarded. All saprolite samples were 5 cm thickness and refer to Table S1 for depths. About 2 kg of saprolite was collected for each sample. Parent granite (~2 kg) was collected from an outcrop near the profile. The saprolites were highly weathered and presented a small number of large grains (maximum diameter ~10 mm) and few primary minerals were observed, with the exception of quartz. Quartz particles could be clearly observed in the saprolite samples, especially in the upper layer of the profile. Furthermore, relatively pure quartz particles (maximum diameter ~5 mm) were also observed on the surface. Two rainwater samples were collected in May and June 2017 in Shenzhen, about 70 km from the saprolite profile sampling site (Fig. 1).

2.2. Analytical methods

Each saprolite sample was homogenized separately in the laboratory after drying. Then, about 50 g of each sample was ground by an agate mill to below 74 μm (passing through a nylon sieve). The granite sample was crushed to less than 2 mm fragments using a hammer before grinding. The sample powder was used to analyze the mineral composition, major and trace elements as well as Li and Nd isotopes. Quartz was separated from saprolite samples before grinding. About 100 g of saprolite sample was successively passed through two nylon sieves with pore sizes of 380 μm and 250 μm, respectively. Then, a sample with sizes between 250 and 380 μm was obtained by selecting pure quartz under a stereo microscope. The separated quartz was immersed in a 5% HNO_3 solution contained in a Teflon beaker and heated on a hot plate (100 °C) for 6 h. After that, the quartz was cleaned with ultra-pure water three times and dried in an oven at 60 °C. Each quartz sample was ground by an agate mill down to below 74 μm and was used to analyze Li concentration and isotopes.

Mineral composition and major elements were determined through X-ray diffraction (XRD) and X-ray fluorescence (XRF) analyses, respectively, at the State Key Laboratory of Biogeology and Environmental Geology, China University of Geosciences, Wuhan. After complete dissolution of the samples with mixture of concentrated HF and HNO_3, trace elements were determined by inductively coupled plasma mass spectrometry (ICP-MS) at the State Key Laboratory of Environmental Geochemistry, Institute of Geochemistry, Chinese Academy of Sciences. Result from XRD analysis provided a mineral percentage estimate for each sample. Chinese national standard samples GBW07103 (granite) and GBW07105 (basalt) were used to calibrate the instrument for the determination of major elements. The international rock standards of AGV-2 and GSP-2 from US Geological Survey (USGS) were analyzed at the same time to ensure the accuracy of trace element determination. Measurement accuracy for most major and trace elements was better than ±5% (2σ) and ±10% (2σ), respectively.

Lithium and Nd isotopes analyses were performed in the State Key Laboratory of Environmental Geochemistry, Institute of Geochemistry, Chinese Academy of Sciences. The method used for the analysis of Li isotopes was described in detail in Zhang et al. (2019) and it was slightly modified for this study. About 50 mg of sample powder was dissolved in a 3 mL mixture of concentrated HF and HNO_3 (3:1, v/v) contained in Savillex screw-top beakers (7 mL) and placed on a hot plate (120 °C, 48 h), followed by refluxing with concentrated HNO_3 and HCl, successively. Subsequently, the sample was re-dissolved in 1 mL 0.40 M HCl for chemical separation. Lithium was purified through a cation exchange column loaded with resin AG 50 W-X12 (200–400 mesh, Bio-Rad) and eluted with 0.40 M HCl. Purification steps were duplicated to ensure that a relatively pure Li solution was obtained. The eluted solution containing Li was evaporated to dryness on a hot plate (120 °C) and re-dissolved in 2% HNO_3 for Li isotope analysis. Ultra-pure water (18.2 MΩ cm) was acquired using a Milli-Q Element system (Millipore, USA). Purification of concentrated HF, HNO_3 and HCl was performed by a DST-1000 acid purification system (Savillex, USA). Lithium isotope ratios were determined by multi-collector ICP-MS (Nu Plasma II). The standard-sample bracketing (SSB) method and the L-SVEC standard (with a Li concentration that is similar to that of the samples: ~80 ng/mL) were used in this study. The external precision (2σ) of this technique, obtained by repeated purification and analysis of seawater samples, was better than ±0.8‰. The measured δ^7Li values of South China Sea seawater samples and international rock standards of AGV-2 and GSP-2 were +31.2 ± 0.8‰ (n = 10), +7.14 ± 0.3‰ (n = 2) and −0.26 ± 0.3‰ (n = 3), respectively, agreeing well with previous δ^7Li values published for these materials (Lin et al., 2016; Li et al., 2019).

Purification of Nd was performed at the Key Laboratory of Marine Chemistry Theory and Technology, Ocean University of China. The same sample dissolution procedure used for Li isotope analysis was followed. Subsequently, Nd was separated from the solutions through the use of two-step chromatographic columns. First, rare-earth elements were separated using a cation exchange column loaded with AG 50 W-X8 resin (100–200 mesh, Bio-Rad). Then, Nd was purified using a chromatographic column with LN-C50-A resin (100–150 mesh, Eichrom Technologies) and eluted with 0.25 M HCl. Neodymium isotope ratios were determined using a multi-collector ICP-MS (Neptune plus) and the accuracy was assessed by running the JNdi-1 standard, which yielded a mean $^{143}Nd/^{144}Nd$ ratio of 0.512094 ± 11 (2σ, n = 8). Samples were corrected for instrumental mass bias using the $^{143}Nd/^{144}Nd$ ratio of 0.7219. The measured $^{143}Nd/^{144}Nd$ ratios for BCR-2 and GSP-2 international rock standards were 0.512639 ± 6 (2σ, n = 2) and 0.511367 ± 6 (2σ, n = 2), respectively. These were comparable with the values of 0.512633 ± 4 (2σ) and 0.511353 ± 4 (2σ) of the two materials from previous studies (Raczek et al., 2003 and references there in).

3. Results

3.1. Mineralogy

Mineral composition of saprolites and parent granite are plotted in Fig. S1. Saprolites were mainly composed of K-feldspar (5%–33%, average 20%), quartz (18%–59%, average 32%), kaolinite (28%–46%, average 37%), and illite (1%–18%, average 10%). Contents of K-feldspar and illite in saprolites were minimal at the surface of the profile and increased with increasing depth. Quartz content was relatively constant in the lower portions of the profile (18%–28%), increasing to its maximum at the surface.

3.2. Major and trace elements

Concentrations of major and trace elements in saprolites and parent granite are summarized in Tables S1 and S2. The chemical index of alteration (CIA) is used to indicate weathering intensity and is defined as the molar ratio of $Al_2O_3/(Al_2O_3+CaO^*+Na_2O + K_2O) \times 100$, where CaO × represents calcium that is not contained in carbonate and phosphate (Nesbitt and Young, 1982). The amount of CaO from apatite was corrected by P_2O_5 content. In the present study, the amount of CaO from carbonate was not corrected because all saprolites had a Ca/Na ratio <1, suggesting that a limited amount of carbonate is present (Rudnick et al., 2004). Thus, CaO values were corrected for apatite but not carbonate for the calculation of CIA values. The CIA value of parent granite was 50, within the range of 45–55 usually found in fresh granites (Nesbitt and Young 1982). In contrast, all saprolite samples had higher CIA values (74–93) than fresh granites. Moreover, these CIA values showed an increasing trend toward the surface (Fig. 2).

In order to quantitatively evaluated the relative depletion or enrichment of mobile elements (e.g., Mg and Li) during chemical weathering of silicates, immobile elements such as Nb, Ta, Zr, Hf, and Ti were selected as the normalization standard (e.g., Middelburg et al., 1988). The parameter tau ($\tau_j = [(C_j/C_i)_w/(C_j/C_i)_p\text{-}1] \times 100$) was defined as relative gain ($\tau_j > 0$) or loss ($\tau_j < 0$) of elements during weathering, where C_j and C_i presented the concentration of mobile (j) and immobile (i) elements, respectively, and "w" and "p" referred to the weathered (w) or parent (p) materials (Chadwick et al., 1990). In the present profile, Ti

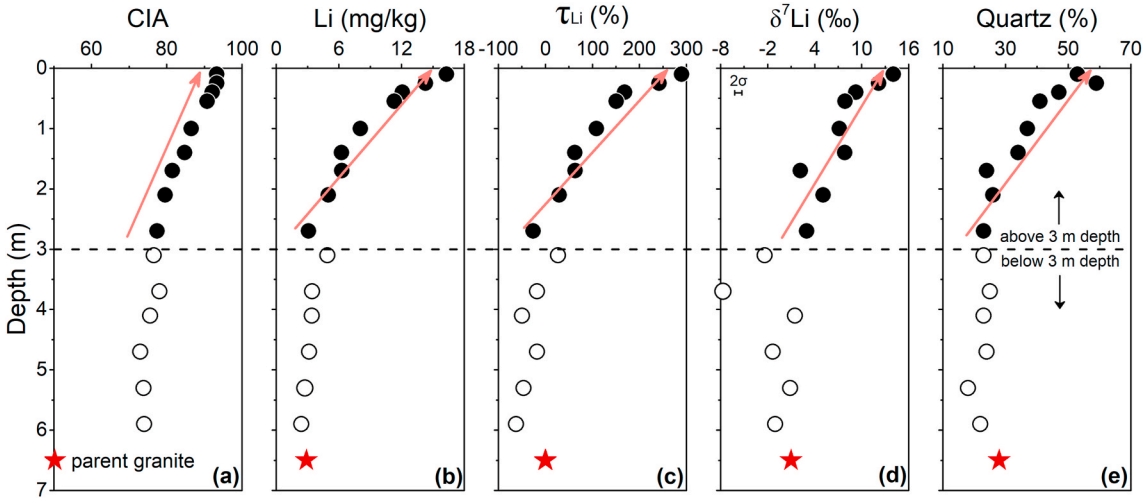

Fig. 2. Depth profile of CIA, [Li], τ_{Li}, δ^7Li, quartz content in the saprolite samples.

was the most immobile element compared with other "immobile elements" (Fig. S2). Therefore, Ti was selected as the normalization standard to calculate τ_j values.

3.3. Nd concentration and isotopic composition

Concentration of Nd in saprolites showed a distinct decreasing trend toward the surface of the profile and kept relatively constant (0.66–1.42 mg/kg) above a depth of 1 m (Fig. 3a and Table S2). The calculated τ_{Nd} values of saprolites were all lower than zero and decreased significantly toward the surface below 3 m, indicating that Nd was leached during the weathering process and almost depleted above 3 m ($\tau_{Nd} < -90\%$) (Fig. 3b). The Nd isotope composition of saprolites ($\varepsilon_{Nd} = -6.1 \pm 0.4$, 1σ) was almost identical to that of parent granite ($\varepsilon_{Nd} = -5.7$) and did not significantly change in the weathering profile (Fig. 3c). Additionally, the ε_{Nd} values of saprolites were significantly higher than those of Chinese loess (-10.6 ± 0.2, 1σ), as well as lower than the mean value of global loess (-10.3 ± 1.2, 1σ) (Li et al., 2009; Chauvel et al., 2014).

3.4. Li concentration and isotopic composition

3.4.1. Saprolite and parent granite

Variations of Li concentration ([Li]) and δ^7Li value in saprolites with profile depth are plotted in Fig. 2. Below a depth of 3 m, all samples had $\tau_j < 0$, except for sample G-10, in contrast, the majority of the samples had $\tau_j > 0$ above 3 m. Moreover, [Li] and τ_j values showed similar trends keeping relatively constant below 3 m, while increasing significantly ([Li]: from 3.1 to 16.3 mg/kg, τ_j: from −26.1% to 289%) toward the surface above this depth. The δ^7Li value of saprolites showed a rough decreasing trend and a significant increasing trend below and above 3 m, respectively. Similar results were observed in a large number of other silicate rock weathering profiles (e.g., Kısakürek et al., 2004; Huh et al., 2004; Ryu et al., 2014). Moreover, the saprolites (+2.2‰ to +14.0‰, average + 7.6‰) above 3 m were distinctly isotopically heavier than that parent granite (+1.0‰).

The relationship between δ^7Li and CIA in saprolites presented two distinctly different groups (Fig. 4). Group 1 showed decreasing δ^7Li with increasing CIA below 3 m, which was similar to the results of Rudnick et al. (2004). In contrast, group 2 showed increasing δ^7Li with increasing CIA above 3 m depth. Additionally, it was worth noting that the δ^7Li

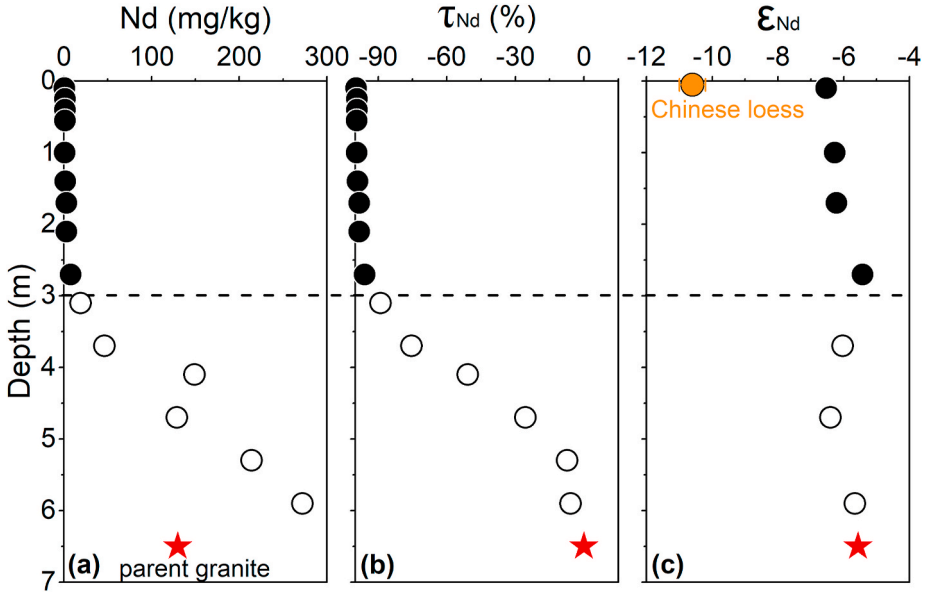

Fig. 3. Depth profile of [Nd], τ_{Nd}, and ε_{Nd} in the saprolites. The ε_{Nd} value of Chinese loess from Li et al. (2009).

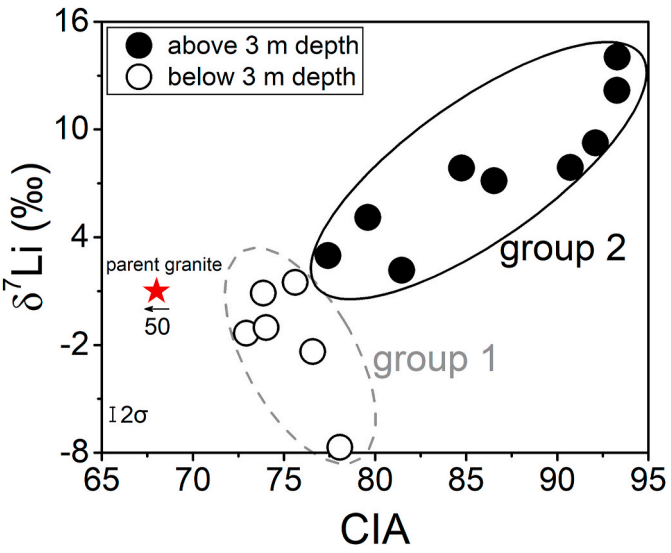

Fig. 4. δ^7Li values vs. CIA along the saprolite profile.

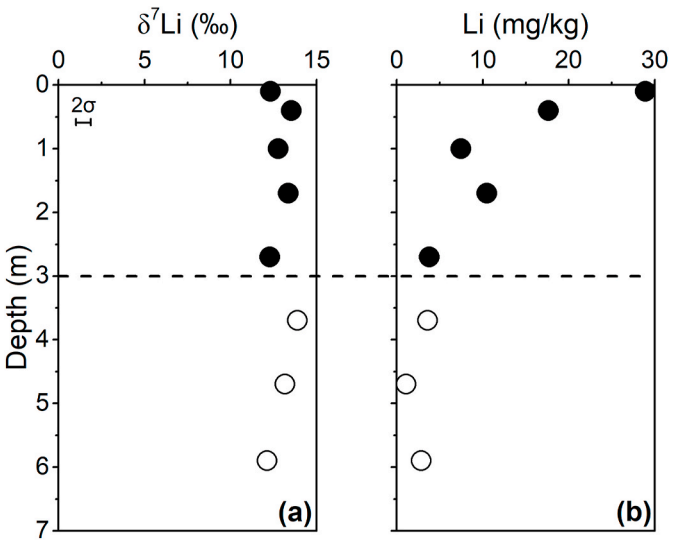

Fig. 6. Depth profile of δ^7Li and [Li] in quartz separated from the saprolites.

value and quartz content showed a good positive correlation ($R^2 = 0.90$, $p < 0.01$) above this depth (Fig. 5b).

3.4.2. Quartz separates from the saprolite samples

Lithium concentration and isotopic composition of quartz separated from saprolites of the profile have been analyzed and presented in Table S2. Lithium concentration of quartz varied greatly from 1.1 to 28.9 mg/kg (average 9.5 mg/kg), and it increased significantly above a depth of 3 m. The δ^7Li of quartz (+12.1‰ to +13.9‰) did not change significantly with the depth of the profile (Fig. 6). Here, the quartz separates were isotopically heavier than bulk saprolite samples and parent granite, as well as isotopically heavier than the upper continental crust (UCC, +0.6 ± 0.6‰, 2σ) and granite worldwide (2.0 ± 2.3‰, 1σ) (Teng et al., 2009; Sauzéat et al., 2015). These observations were consistent with the results from previous studies revealing that quartz tends to be isotopically heavy and it may have a relatively high Li concentration (Lynton et al., 2005; Teng et al., 2006a; Sun et al., 2016; Li et al., 2018; Zhang et al., 2021a) (Fig. 7).

The mineral composition of the saprolite is divided into two parts that is quartz and the rest of minerals assemblage (RMA). Accordingly, the amount of Li and δ^7Li in bulk sprolites contributed from quartz and RMA was calculated (Eq. 1 to Eq. 5, Appendix) and presented in Fig. 8. The saprolite Li was mainly found in RMA, with the exception of near the surface layer. The percentage of Li contributed from quartz ($P_{Li-C\text{-}quartz}$ for short) varied from 8.3% to 26% below 3 m and increased from 28% to 94% towards surface above 3 m. The value of δ^7Li in RMA (δ^7Li_{RMA}) showed a decreasing and increasing trend towards surface blow and above 3 m, respectively. The saprolite δ^7Li contributed from quartz ($\delta^7Li_{C\text{-}quartz}$) did not change much below 3 m (+1.1‰ to +3.6‰) and reached the maximum (+11.6‰) near the surface.

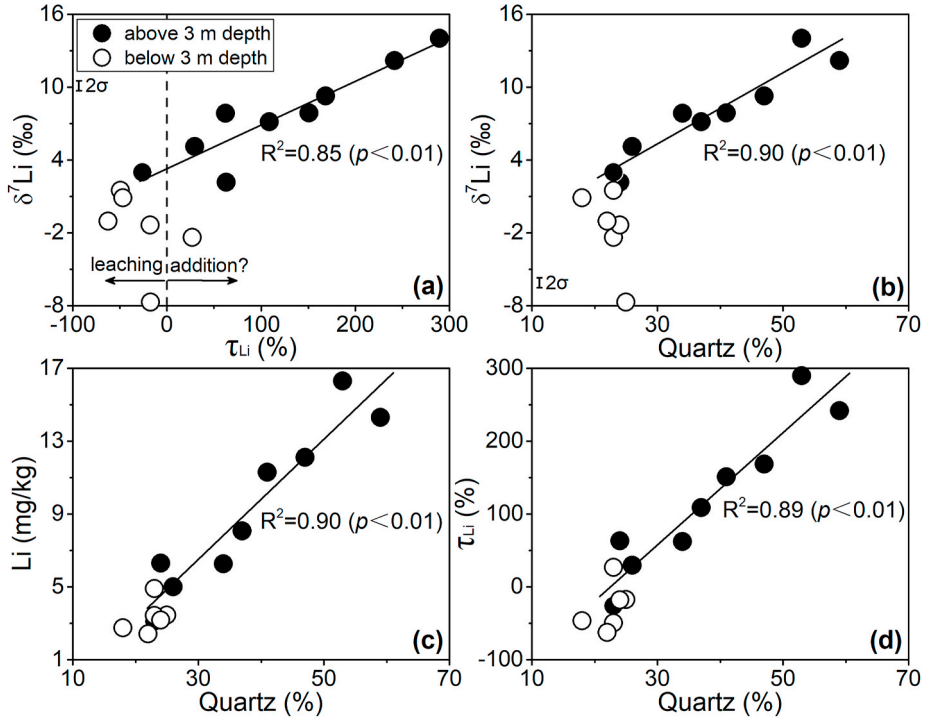

Fig. 5. The relationship between δ^7Li and τ_{Li}, quartz and δ^7Li (and [Li], τ_{Li}) in the saprolite samples. Correlation analysis is the data points above 3 m depth.

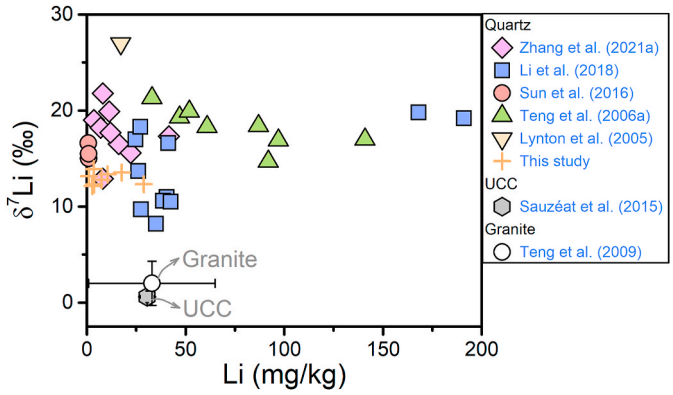

Fig. 7. δ^7Li values vs. [Li] in quartz, granite and the UCC.

3.5. Rain water

Lithium concentration and isotopic composition of two unfiltered rainwater samples (SZ-1 and SZ-2) were 0.78 and 0.86 μg/L, +6.1‰ and +9.1‰, respectively. The δ^7Li values were close to those measured in unfiltered (+10.2‰) and filtered (+14.3‰) rainwater samples from Hawaii (Pistiner and Henderson, 2003). Meanwhile, the values fell within the range of +3.2‰ to +34.1‰ reported in rainwater samples from France which was not affected by anthropogenic sources (Millot et al., 2010).

4. Discussion

In the present profile, above 3 m, the saprolites were characterized by that Li was isotopically heavier than the parent granite. Moreover, the δ^7Li value of saprolites showed a distinct increasing trend toward the surface above a depth of 3 m. Factors that may affect Li isotope composition in saprolites are discussed here, such as formation of secondary minerals, input of externally-derived Li, and relative quartz enrichment.

4.1. Formation of secondary minerals

Below a depth of 3 m, the δ^7Li values of saprolites were almost all lower than those of parent granite and showed a decreasing trend toward the surface of the profile (Fig. 2d). Moreover, the rough negative correlation between CIA and δ^7Li (group 1, Fig. 4) suggested that saprolites become isotopically lighter as weathering progresses (Rudnick et al., 2004). This was consistent with previous studies that revealed that the lighter ^{6}Li tends to be retained in weathered products during weathering processes, due to the fact that the lighter ^{6}Li was preferentially partitioned into newly formed secondary minerals, such as clays and metal oxyhydroxides. Experimental results suggested that significant isotopic fractionation occurred during the two processes of Li sorption onto surface and incorporation into the crystal structure (octahedral sites) of secondary minerals, such as gibbsite, kaolinite, vermiculite (Zhang et al., 1998; Zhang et al., 2021b; Wimpenny et al., 2015; Li and Liu, 2020). In the present study, clay minerals (kaolinite + illite) content in saprolites increased as weathering progresses and correlated negatively with δ^7Li values below 3 m (Fig. S3), suggesting that the formation of clay minerals may be responsible for the relative enrichment of ^{6}Li in these saprolites.

During the weathering process, Li is gradually leached out and its isotopes are fractionated. However, it is worth noting that sample G-11 presented the lightest Li isotope (δ^7Li = −7.7‰) but showed limited Li depletion (τ_{Li} = −17.5%), a phenomenon that would require extremely low α values to be explained. Furthermore, an anomaly emerged from the analysis of sample G-10, which appeared relatively enriched in ^{6}Li (δ^7Li = −2.4‰) but was added Li (τ_{Li} = 26.9%). This phenomenon could not be accounted by the process known as Rayleigh distillation but it may be due to the occurrence of intermixing with isotopically light Li materials (Rudnick et al., 2004). The isotopically light materials may derive from the upper layer of the profile. Below 3 m depth, the rough negatively relationship between τ_{Li} and δ^7Li and the δ^7Li value decreased toward the surface support this speculation (Figs. 2c and 5a). Potentially, the portion of micron-sized particles, which was intensively weathered and had a lower δ^7Li value in the upper layer, could be transported downward along with the fluid. Similar results have been observed in studies on B, Fe, and Mg isotopes geochemical behavior during weathering processes at Shale Hills Critical Zone Observatory

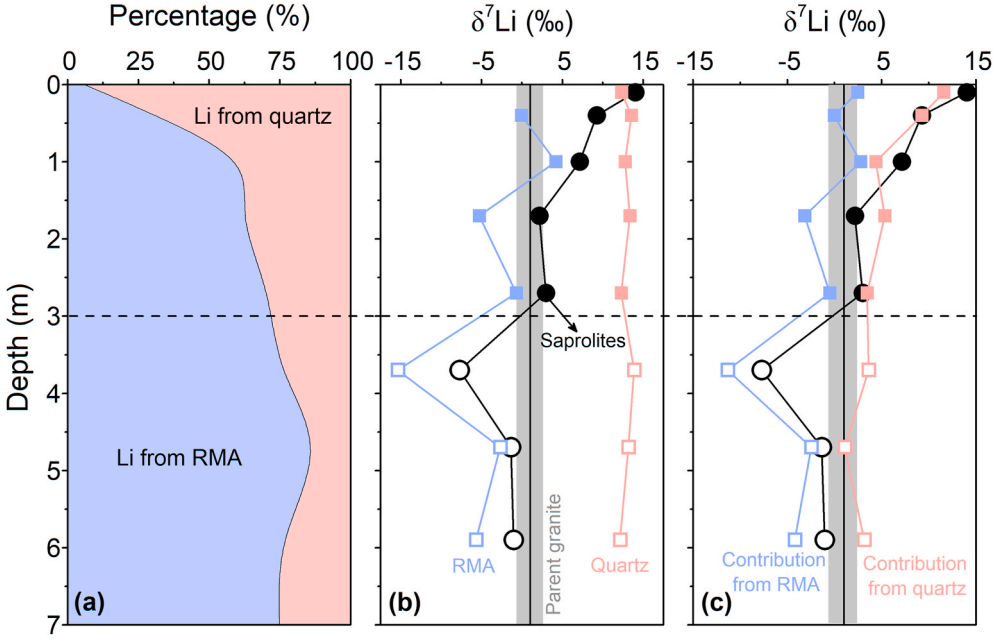

Fig. 8. Depth profile of (a) the percentage of Li contribution from quartz and the rest of minerals assemblage (RMA), (b) δ^7Li value in bulk saprolite samples, quartz, and RMA, (c) δ^7Li value of saprolites contributes from quartz and RMA.

(Yesavage et al., 2012; Noireaux et al., 2014; Ma et al., 2015). Another possibility was the preferential release of ^{6}Li in the upper saprolites during clay alteration or dissolution of saprolites with low $\delta^{7}Li$ (Ryu et al., 2014). As a result, more ^{6}Li also migrated downward leading to relative enrichment of the lower layer.

4.2. Input of externally-derived Li

Above a depth of 3 m, the $\delta^{7}Li$ values of saprolites were higher than those of parent granite and showed an increasing trend toward the surface of the profile (Fig. 2d). Similar results were observed in [Li] and τ_{Li} values of the present profile (Fig. 2b and c). This seems to contradict with the general assumption that Li is leached and lighter ^{6}Li is preferentially retained in weathered products during silicate weathering processes (e.g., Rudnick et al., 2004; Liu et al., 2013). Previous studies suggested that addition of externally-derived Li via precipitation and eolian deposition could be the main cause of the increase in $\delta^{7}Li$ value and/or [Li] in the upper layer of the weathering profile (e.g., Pistiner and Henderson, 2003; Kısakürek et al., 2004; Huh et al., 2004; Liu et al., 2013; Li et al., 2020). However, these scenarios could not fit the profile of this study.

Generally, the $\delta^{7}Li$ value of rainwater, especially when it is mixed with marine aerosols ($\delta^{7}Li = +31.5‰$), is significantly higher than that of weathering products (e.g., Pistiner and Henderson, 2003; Huh et al., 2004). As a result, the addition of rainwater Li will lead to an increase of τ_{Li} and $\delta^{7}Li$ values in saprolites near the surface layer (Huh et al., 2004). In the present profile, although the exposure time of the parent granite was not known, it can be estimated as greater than 0.2 Ma (depth of 6 m and not reaching the fresh granite) using the granite erosion rate of ~30 m/Ma from our pervious study in Longnan, a location with climatic conditions similar to those in this study site (distance ~180 km) (Cui et al., 2016). Therefore, rainwater would introduce ~31.2 mg Li per cm^{2} (0.82 ng/cm^{3} × 190 cm/yr × 2 × 10^{5} yr) to the profile according to the calculation method adopted from Pistiner and Henderson (2003). As a result, the average [Li] of saprolites should be increased by a net addition of 34.7 mg/kg. In addition, the $\delta^{7}Li$ value of rainwater samples (+6.1‰ and +9.1‰) is distinctly higher than that of the parent granite (+1.0‰). These results seemed to support the assumption that addition of rainwater Li resulted in an increase in [Li] in the upper layer of the profile. However, the average [Li] was only 6.6 mg/kg in the saprolite samples, suggesting that the greater proportion of rainwater Li was not retained but it flowed away. The most important is that the $\delta^{7}Li$ value of the unfiltered rainwater samples is distinctly lower than that of saprolites near the surface layer (maximum +14.0‰). Although the filtered rainwater may have relatively higher $\delta^{7}Li$ value, the unfiltered rainwater samples represent the total wet precipitation of Li which is mixed with the upper saprolties. Therefore, the input of rainwater Li may contribute to the increase of [Li] and $\delta^{7}Li$ in the saprolites, but it cannot explain the very high $\delta^{7}Li$ value in the upper layer.

Generally, [Li] and $\delta^{7}Li$ of eolian depositions are close to those of the UCC (30.5 ± 3.6 (2σ) mg/kg and +0.6 ± 0.6‰ (2σ)). Loess is a typical eolian deposition with relatively high [Li] (16.6–61.3 mg/kg, average 37.8 mg/kg) and a narrow range of $\delta^{7}Li$ values (−2.9‰–+4.7‰, average + 0.75‰) was reported around the world (Sauzéat et al., 2015 and references therein). As a potential source of externally-derived Li, eolian depositions have a higher [Li] than that found in saprolites, but they present a distinctly lower $\delta^{7}Li$ value. Thus, the eolian depositions cannot explain the presence of extremely high $\delta^{7}Li$ values in the present profile. Moreover, the $\delta^{7}Li$ of the eolian depositions will further decreases (not increases) during post-depositional chemical weathering. Additionally, the Nd isotopes are used to trace the sources of materials, such as eolian dust (e.g., Rao et al., 2008). Analyses revealed that there are no abundant eolian depositions incorporated in the profile as supported by that the Nd isotope composition (ε_{Nd}) of the saprolites was almost identical to that of parent granite (Fig. 3c). In summary, there was no evidence that eolian depositions were the main reason for the elevated [Li] and $\delta^{7}Li$ value in the upper saprolites of the present profile.

4.3. Evidence of ^{7}Li enrichment in the upper saprolites due to relative enrichment of quartz

Quartz may gradually be enriched in weathering products as granite weathering progresses, because quartz is a major rock-forming mineral found in granite and is relatively resistant to chemical weathering. In this study, the enrichment of quartz observed in highly weathered saprolties was in line with this speculation (Fig. 2e). Similar results were observed in other granite weathering profiles from southern China, but not in the surface layer where dissolution of quartz was caused by more intense weathering conditions (Liu et al., 2016; Fu et al., 2019).

We speculated that the relative enrichment of quartz contributed significantly to the increase of [Li] and $\delta^{7}Li$ in the upper saprolites. The direct evidence was that Li was abundant and distinctly isotopically heavier in quartz separated from the saprolites (Fig. 6). Moreover, quartz content correlated positively with [Li] ($R^{2} = 0.90$, $p < 0.01$) and $\delta^{7}Li$ ($R^{2} = 0.90$, $p < 0.01$) in saprolites above 3 m (Fig. 5), which supported this speculation. Similar results were observed in upper saprolites developed on basalt (Huh et al., 2004; Liu et al., 2013), however quartz (or quartz + mica) was used as a proxy for the input of externally-derived materials (e.g., dust) because a limited amount of quartz present in the basalt. In the present study, quartz contained in saprolites was mainly due to the weathering of granite rather than to externally-derived materials (see section 4.2). Moreover, a great proportion of large quartz fragments (maximum diameter ~5 mm) observed in the saprolites did not derive from eolian deposition. In order to evaluate the contributions of quartz to [Li] and $\delta^{7}Li$ of saprolites, an approach based on two end-member components (quartz and the rest of minerals assemblage (RMA)) was adopted and the calculated results suggested that the total Li contained in saprolites from quartz contribution increased toward the surface and accounted for a very high proportion of this element near the surface layer (Fig. 8a). As a result, above 3 m, the calculated contribution of $\delta^{7}Li$ from quartz increased toward the surface and was close to the $\delta^{7}Li$ values in saprolites (Fig. 8c), suggesting that enrichment of quartz was the main cause of the elevated $\delta^{7}Li$ in upper saprolites. Due to $\delta^{7}Li$ in quartz is about +13‰, a 10% increase of Li from quartz will result in a +1.3‰ increase of $\delta^{7}Li$ in the studied saprolites.

Furthermore, most of the calculated $\delta^{7}Li$ values in the rest of minerals assemblage (RMA) were lower than those of parent granite (Fig. 8b). This was due to the RMA containing a significant proportion of secondary clays (e.g., kaolinite) (Fig. S1), which tended to incorporated ^{6}Li (Liu et al., 2013). It is worth noting that the calculated $\delta^{7}Li$ of the upper RMA was higher than that of the lower RMA and was close to that of parent granite. One explanation is that rainwater Li with a higher $\delta^{7}Li$ is added to the upper saprolites (Huh et al., 2004). However, the difference was that most of the τ_{Li} values calculated based on Li content from the RMA alone was lower than zero, suggesting Li was leached from the RMA rather than added to in the present profile. We speculate that this may be due to the release of ^{6}Li from the upper RMA via transport of micron-sized particles and/or alteration or dissolution of saprolites, resulting in the $\delta^{7}Li$ vaule being higher in the upper RMA than in the lower RMA. This deduction is consistent with the fact that saprolites was present the lightest Li isotope near the 3 m depth layer, but received additional Li (see section 4.1). Accordingly, the $\delta^{7}Li$ value in the RMA was control by the formation of secondary clays, as well as by the redistribution of Li vertically along the profile.

Interestingly, most of τ_{Li} value were greater than zero and showed an increasing trend toward the surface above 3 m (Fig. 2c), indicating that Li was added to the saprolites instead of leaching away. However, as previously mentioned (see section 4.2), there was little contribution of Li from externally-derived materials for the saprolites. This observation could be attributed to the significant increase in [Li] in quartz above 3 m (Fig. 6b). For the surface layer samples G-1 and G-2, the τ_{Li} values

calculated based on Li content from quartz alone were 266 and 84, respectively. Therefore, the "additional Li" found in the saprolites was mainly due to an increase in [Li] in quartz from the upper layer. However, what confusing is that [Li] in quartz varied greatly in the upper saprolites and was characterized by a gradual increase toward the surface (from 3.8 to 28.9 mg/kg), while the δ^7Li value kept relatively constant across the profile (Fig. 6). In the low temperature environment, Li is difficult to incorporate into quartz due to it has a relatively stable structure. Experimental results suggested that in the high temperature and high pressure conditions, Li can be incorporated into the structure of quartz though a coupled substitution of Si^{4+} with $Li^{+}+Al^{3+}$ (Lynton et al., 2005). Thus, it can be speculated that the large variation in Li concentration in quartz may occur during granite petrogenesis rather than the later weathering process. The crystallization temperature of granitic system may affect the variation of [Li] in quartz during petrogenesis process (Larsen et al., 2004). However, this temperature should not be significantly different at a very small scale, which cannot explain the observations in this study. Previous study suggested that the diffusion of Li generally resulted in a large variation in [Li] and δ^7Li in rocks of the contact zone between pegmatite and amphibolite (and schist) (Teng et al., 2006b). However, the relatively constant δ^7Li value in quartz does not seem to support this possibility. This anomalous observation in this study remains enigmatic. Regardless of the cause(s) for the extreme variation of [Li] in quartz, the fact is that relatively high [Li] and δ^7Li in quartz may cause a significant increase in δ^7Li in saprolites developed on granite.

In summary, the variation of δ^7Li values in saprolites resulted from combined effects of dissolution, leaching and reintroduction between secondary minerals and water (e.g., Liu et al., 2013), and also from the changes in the content of inert Li-containing minerals, such as quartz. In the present study, Li isotope composition in saprolites developed on granite was mainly controlled by the percentage of Li from secondary clays (low δ^7Li) and quartz (high δ^7Li).

5. Conclusion

Lithium isotope composition was carefully investigated in highly weathered saprolites developed on granite from Huizhou, southern China. Saprolites were isotopically lighter than parent granite in the lower layer of the weathering profile, while they were isotopically heavier in the upper layer. Formation of secondary minerals (such as kaolinite) may be a significant factor for the relative enrichment of lighter ^{6}Li in saprolites below 3 m. Moreover, more ^{6}Li migrated downward from the upper layer and relatively enrichment in the lower layer may also be responsible for the low δ^7Li value observed in the lower saprolites. Above 3 m, relative quartz enrichment contributed significantly to the increase of δ^7Li in the saprolites. The results of this study suggested that a 10% increase in Li from quartz enrichment produced a +1.3‰ increase of δ^7Li in the saprolites. In summary, Li isotope composition in the saprolite samples was mainly controlled by the percentage of Li derived from secondary clays (low δ^7Li) and quartz (high δ^7Li), as well as by the redistribution of Li in the vertically along the profile, while the input of externally-derived Li contributed little to the isotopic composition.

Declaration of competing interest

The authors declare that they have no known competing financial interests or personal relationships that could have appeared to influence the work reported in this paper.

Acknowledgements

We are grateful to Associate Editor Gong Qingjie and two anonymous reviews for their constructive comments. We thank Dr. He Hui-Jun for helping us separating Nd from saprolite and granite samples, and Xia Ke for helping us collecting rainwater samples. This work was supported jointly by the National Natural Science Foundation of China (No. 41930863, 42003007), and the Second Tibetan Plateau Scientific Expedition and Research (2019QZKK0707), and Special Fund for Basic Scientific Research of Central Colleges, Chang'an University (No. 3001102278302).

Appendix A. Supplementary data

Supplementary data to this article can be found online at https://doi.org/10.1016/j.apgeochem.2020.104825.

References

Chadwick, O.A., Brimhall, G.H., Hendricks, D.M., 1990. From a black to a gray box—a mass balance interpretation of pedogenesis. Geomorphology 3 (3–4), 369–390.
Chauvel, C., Garçon, M., Bureau, S., Besnault, A., Jahn, B.M., Ding, Z., 2014. Constraints from loess on the Hf–Nd isotopic composition of the upper continental crust. Earth Planet Sci. Lett. 388, 48–58.
Cui, L.F., Liu, C.Q., Xu, S., Zhao, Z.Q., Liu, T.Z., Liu, W.J., Zhang, Z.J., 2016. Subtropical denudation rates of granitic regolith along a hill ridge in Longnan, SE China derived from cosmogenic nuclide depth-profiles. J. Asian Earth Sci. 117, 146–152.
Fu, W., Li, X., Feng, Y., Feng, M., Peng, Z., Yu, H., Lin, H., 2019. Chemical weathering of S-type granite and formation of Rare Earth Element (REE)-rich regolith in South China: Critical control of lithology. Chem. Geol. 520, 33–51.
Hindshaw, R.S., Tosca, R., Goût, T.L., Farnan, I., Tosca, N.J., Tipper, E.T., 2019. Experimental constraints on Li isotope fractionation during clay formation. Geochem. Cosmochim. Acta 250, 219–237.
Huh, Y., Chan, L.H., Zhang, L., Edmond, J.M., 1998. Lithium and its isotopes in major world rivers: implications for weathering and the oceanic budget. Geochem. Cosmochim. Acta 62 (12), 2039–2051.
Huh, Y., Chan, L.H., Edmond, J.M., 2001. Lithium isotopes as a probe of weathering processes: orinoco River. Earth Planet Sci. Lett. 194 (1–2), 189–199.
Huh, Y., Chan, L.H., Chadwick, O.A., 2004. Behavior of lithium and its isotopes during weathering of Hawaiian basalt. Geochem. Geophys. Geosyst. 5 (9).
Kısakürek, B., Widdowson, M., James, R.H., 2004. Behaviour of Li isotopes during continental weathering: the Bidar laterite profile, India. Chem. Geol. 212 (1–2), 27–44.
Kısakürek, B., James, R.H., Harris, N.B.W., 2005. Li and δ^7Li in Himalayan rivers: proxies for silicate weathering?[J]. Earth Planet Sci. Lett. 237 (3–4), 387–401.
Kuang, J., Qi, S., Wang, S., Xiao, Z., Zhang, M., Zhao, X., 2019. The granite intrusion in Huizhou, Guangdong province and its geothermal implication. Earth Sci. 1–23 (in Chinese with English abstract).
Larsen, R.B., Henderson, I., Ihlen, P.M., Jacamon, F., 2004. Distribution and petrogenetic behaviour of trace elements in granitic pegmatite quartz from South Norway. Contrib. Mineral. Petrol. 147 (5), 615–628.
Lemarchand, E., Chabaux, F., Vigier, N., Millot, R., Pierret, M.C., 2010. Lithium isotope systematics in a forested granitic catchment (Strengbach, Vosges Mountains, France). Geochem. Cosmochim. Acta 74, 4612–4628.
Lehmann, K., Pettke, T., Ramseyer, K., 2011. Significance of trace elements in syntaxial quartz cement, Haushi Group sandstones, Sultanate of Oman. Chem. Geol. 280 (1–2), 47–57.
Li, G., Chen, J., Ji, J., Yang, J., Conway, T.M., 2009. Natural and anthropogenic sources of East Asian dust. Geology 37 (8), 727–730.
Li, J., Huang, X.L., Wei, G.J., Liu, Y., Ma, J.L., Han, L., He, P.L., 2018. Lithium isotope fractionation during magmatic differentiation and hydrothermal processes in rare-metal granites. Geochem. Cosmochim. Acta 240, 64–79.
Li, W., Liu, X.M., Godfrey, L.V., 2019. Optimisation of lithium chromatography for isotopic analysis in geological reference materials by MC-ICP-MS. Geostand. Geoanal. Res. 43 (2), 261–276.
Li, W., Liu, X.M., Chadwick, O.A., 2020. Lithium isotope behavior in Hawaiian regoliths: soil-atmosphere-biosphere exchanges. Geochem. Cosmochim. Acta 285, 175–192.
Li, W., Liu, X.M., 2020. Experimental investigation of lithium isotope fractionation during kaolinite adsorption: implications for chemical weathering. Geochem. Cosmochim. Acta 284, 156–172.
Lin, J., Liu, Y., Hu, Z., Yang, L., Chen, K., Chen, H., Zong, K., Gao, S., 2016. Accurate determination of lithium isotope ratios by MC-ICP-MS without strict matrix-matching by using a novel washing method. J. Anal. At. Spectrom. 31 (2), 390–397.
Liu, X.M., Rudnick, R.L., McDonough, W.F., Cummings, M.L., 2013. Influence of chemical weathering on the composition of the continental crust: insights from Li and Nd isotopes in bauxite profiles developed on Columbia River Basalts. Geochem. Cosmochim. Acta 115, 73–91.
Liu, W., Liu, C., Brantley, S.L., Xu, Z., Zhao, T., Liu, T., Yu, C., Xue, D., Zhao, Z., Cui, L., Zhang, Z., Fan, B., Gu, X., 2016. Deep weathering along a granite ridgeline in a subtropical climate. Chem. Geol. 427, 17–34.
Lynton, S.J., Walker, R.J., Candela, P.A., 2005. Lithium isotopes in the system Qz-Ms-fluid: an experimental study. Geochem. Cosmochim. Acta 69 (13), 3337–3347.
Ma, L., Teng, F.Z., Jin, L., Ke, S., Yang, W., Gu, H.O., Brantley, S.L., 2015. Magnesium isotope fractionation during shale weathering in the Shale Hills Critical Zone Observatory: accumulation of light Mg isotopes in soils by clay mineral transformation. Chem. Geol. 397, 37–50.
Myers, J.S., 1997. Geology of granite. J. Roy. Soc. West Aust. 80, 87.

Middelburg, J.J., van der Weijden, C.H., Woittiez, J.R., 1988. Chemical processes affecting the mobility of major, minor and trace elements during weathering of granitic rocks. Chem. Geol. 68 (3–4), 253–273.

Millot, R., Petelet-Giraud, E., Guerrot, C., Négrel, P., 2010. Multi-isotopic composition (δ^7Li–δ^{11}B–δD–δ^{18}O) of rainwaters in France: origin and spatio-temporal characterization. Appl. Geochem. 25 (10), 1510–1524.

Nesbitt, H., Young, G.M., 1982. Early Proterozoic climates and plate motions inferred from major element chemistry of lutites. Nature 299, 715.

Négrel, P., Millot, R., 2019. Behaviour of Li isotopes during regolith formation on granite (Massif Central, France): controls on the dissolved load in water, saprolite, soil and sediment. Chem. Geol. 523, 121–132.

Noireaux, J., Gaillardet, J., Sullivan, P.L., Brantley, S.L., 2014. Boron isotope fractionation in soils at Shale Hills CZO. Procedia Earth Planet. Sci. 10, 218–222.

Pistiner, J.S., Henderson, G.M., 2003. Lithium-isotope fractionation during continental weathering processes. Earth Planet Sci. Lett. 214, 327–339.

Pogge von Strandmann, P.A.E., Burton, K.W., James, R.H., van Calsteren, P., Gíslason, S. R., Mokadem, F., 2006. Riverine behaviour of uranium and lithium isotopes in an actively glaciated basaltic terrain. Earth Planet Sci. Lett. 251 (1–2), 134–147.

Pogge von Strandmann, P.A.E., Henderson, G.M., 2015. The Li isotope response to mountain uplift. Geology 43 (1), 67–70.

Rao, W., Chen, J.U.N., Yang, J., Ji, J., Li, G., Tan, H., 2008. Sr-Nd isotopic characteristics of eolian deposits in the Erdos Desert and Chinese Loess Plateau: implications for their provenances. Geochem. J. 42 (3), 273–282.

Raczek, I., Jochum, K.P., Hofmann, A.W., 2003. Neodymium and strontium isotope data for USGS reference materials BCR-1, BCR-2, BHVO-1, BHVO-2, AGV-1, AGV-2, GSP-1, GSP-2 and eight MPI-DING reference glasses. Geostand. Newsl. 27 (2), 173–179.

Rudnick, R.L., Tomascak, P.B., Njo, H.B., Gardner, L.R., 2004. Extreme lithium isotopic fractionation during continental weathering revealed in saprolites from South Carolina. Chem. Geol. 212 (1–2), 45–57.

Ryu, J.S., Vigier, N., Lee, S.W., Lee, K.S., Chadwick, O.A., 2014. Variation of lithium isotope geochemistry during basalt weathering and secondary mineral transformations in Hawaii. Geochem. Cosmochim. Acta 145, 103–115.

Sauzéat, L., Rudnick, R.L., Chauvel, C., Garçon, M., Tang, M., 2015. New perspectives on the Li isotopic composition of the upper continental crust and its weathering signature. Earth Planet Sci. Lett. 428, 181–192.

Schauble, E.A., 2004. Applying stable isotope fractionation theory to new systems. Rev. Mineral. Geochem. 55 (1), 65–111.

Sun, H., Gao, Y., Xiao, Y., Gu, H.O., Casey, J.F., 2016. Lithium isotope fractionation during incongruent melting: constraints from post-collisional leucogranite and residual enclaves from Bengbu Uplift, China. Chem. Geol. 439, 71–82.

Teng, F.Z., McDonough, W.F., Rudnick, R.L., Walker, R.J., Sirbescu, M.L.C., 2006a. Lithium isotopic systematics of granites and pegmatites from the Black Hills, South Dakota. Am. Mineral. 91 (10), 1488–1498.

Teng, F.Z., McDonough, W.F., Rudnick, R.L., Walker, R.J., 2006b. Diffusion-driven extreme lithium isotopic fractionation in country rocks of the Tin Mountain pegmatite. Earth Planet Sci. Lett. 243 (3–4), 701–710.

Teng, F.Z., Rudnick, R.L., McDonough, W.F., Wu, F.Y., 2009. Lithium isotopic systematics of A-type granites and their mafic enclaves: further constraints on the Li isotopic composition of the continental crust. Chem. Geol. 262, 370–379.

Teng, F.Z., Li, W.Y., Rudnick, R.L., Gardner, L.R., 2010. Contrasting lithium and magnesium isotope fractionation during continental weathering. Earth Planet Sci. Lett. 300 (1–2), 63–71.

Tomascak, P.B., Magna, T., Dohmen, R., 2016. Advances in Lithium Isotope Geochemistry. Springer, Berlin.

Vigier, N., Decarreau, A., Millot, R., Carignan, J., Petit, S., France-Lanord, C., 2008. Quantifying Li isotope fractionation during smectite formation and implications for the Li cycle. Geochem. Cosmochim. Acta 72 (3), 780–792.

Wimpenny, J., Colla, C.A., Yu, P., Yin, Q.Z., Rustad, J.R., Casey, W.H., 2015. Lithium isotope fractionation during uptake by gibbsite. Geochem. Cosmochim. Acta 168, 133–150.

Williams, L.B., Hervig, R.L., 2005. Lithium and boron isotopes in illite-smectite: the importance of crystal size. Geochem. Cosmochim. Acta 69, 5705–5716.

Yamaji, K., Makita, Y., Watanabe, H., Sonoda, A., Kanoh, H., Hirotsu, T., Ooi, K., 2001. Theoretical estimation of lithium isotopic reduced partition function ratio for lithium ions in aqueous solution. J. Phys. Chem. 105 (3), 602–613.

Yesavage, T., Fantle, M.S., Vervoort, J., Mathur, R., Jin, L., Liermann, L.J., Brantley, S.L., 2012. Fe cycling in the Shale Hills Critical Zone Observatory, Pennsylvania: an analysis of biogeochemical weathering and Fe isotope fractionation. Geochem. Cosmochim. Acta 99, 18–38.

Zhang, L., Chan, L.H., Gieskes, J.M., 1998. Lithium isotope geochemistry of pore waters from ocean drilling program sites 918 and 919, irminger basin. Geochem. Cosmochim. Acta 62, 2437–2450.

Zhang, J.W., Meng, J.L., Zhao, Z.Q., Liu, C.Q., 2019. Accurate determination of lithium isotopic compositions in geological samples by multi-collector inductively coupled plasma-mass spectrometry. Chin. J. Anal. Chem. 47 (3), 415–422.

Zhang, J.W., Zhao, Z.Q., Yan, Y.N., Cui, L.F., Wang, Q.L., Meng, J.L., Li, X.D., Liu, C.Q., 2021a. Lithium and its isotopes behavior during incipient weathering of granite in the eastern Tibetan Plateau. China. Chem. Geol. 559, 119969.

Zhang, X.Y., Saldi, G.D., Schott, J., Bouchez, J., Kuessner, M., Montouillout, V., Henehan, M., Gaillardet, J., 2021b. Experimental constraints on Li isotope fractionation during the interaction between kaolinite and seawater. Geochim. Cosmochim. Acta 292, 333–347.